

## Single-atom dynamics revealed by photon correlations

V. Gomer, F. Strauch, B. Ueberholz, S. Knappe, and D. Meschede  
*Institut für Angewandte Physik, Universität Bonn, Wegelerstrasse 8, D-53115 Bonn, Germany*  
 (Received 6 October 1997)

We have studied a single neutral atom stored in a magneto-optical trap by recording arrival times of fluorescence photons emitted by the atom. Photon correlations at nanosecond scales (Rabi oscillations), at microseconds (intensity and polarization correlations), and also at milliseconds (position correlations) reveal the dynamical behavior of the atomic excitation, of the atomic orientation, and of its transport in the trap at both the optical wavelength scale and the trap size. [S1050-2947(98)50109-6]

PACS number(s): 32.80.Pj, 42.50.Vk, 42.50.Ar

Fluorescence emitted by laser-cooled atoms provides valuable information for a noninvasive study of the atomic dynamics in laser fields. If many atoms are observed, their fluorescence can fluctuate due to beating of the Doppler-shifted light from different atoms. This idea was used to study atomic transport in a standing laser field on the scale of the optical wavelength [1] and for spectral analysis of scattered light from atoms in optical molasses [2] by analyzing intensity correlations. Another application of the intensity correlation technique is the observation of nonclassical behavior in the resonance fluorescence, e.g., photon antibunching [3]. In such experiments intensity fluctuations are caused by a one-atom effect, by time dependence of the atomic excitation in the light field (Rabi oscillations). The presence of several atoms or, even worse, fluctuations of the atom number in the observation region leads to a smearing out of the correlation signal. This makes a single trapped ion the best experimental choice [3]. Trapping of individual ions was accomplished a long time ago [4], but only recently has it been for neutral atoms [5]. Using a standard magneto-optical trap (MOT) [6], which is loaded from a cesium background vapor, we study fluorescence fluctuations from a single trapped atom.

We will show here that single-atom trapping causes atomic dynamics to manifest itself in fluorescence fluctuations at all relevant time scales. At the shortest time scale (nanoseconds) we have found intensity correlations in the form of Rabi oscillations. The Rabi frequency is a measure of the interaction strength of the local electric field and the atomic dipole and gives direct access to the internal dynamics of the atom. At a microsecond time scale additional intensity fluctuations (and also polarization fluctuations observed in [1]) become visible. These are induced by atomic motion through the standing light fields. At even larger times, atomic transport up to macroscopic (trap size) scales can be studied, provided that photon detection is spatially resolved [7]. Thus a single simple method allows us to analyze both qualitatively and quantitatively the details of the atom-field interaction in a self-consistent manner.

The intensity correlation function defined classically in terms of the fluorescence intensity  $I(t)$  is given by

$$g^{(2)}(\tau) = \frac{\langle I(t)I(t+\tau) \rangle}{\langle I(t) \rangle^2}, \quad (1)$$

where  $\langle \rangle$  denotes an average over time. In the photon language,  $g^{(2)}(\tau)$  describes the conditional probability of detecting a second photon at time  $t+\tau$  after a first one is observed at  $t$  [8]. In few-atom experiments fluorescence is usually collected from a large solid angle. As a result many Fresnel (coherence) zones are observed and interference effects of light fields from different atoms vanish. Thus the photon coincidence number from  $N$  atoms detected in channel  $\tau$  is proportional to [9]

$$Ng^{(2)}(\tau) + N(N-1), \quad (2)$$

with a transparent meaning: the probability of detecting a coincidence (two photons) from one and the same atom is proportional to  $N$  and their eventual correlation is described by  $g^{(2)}(\tau)$ . Additionally one has occasional coincidences of two uncorrelated photons from two different atoms. The contrast of the signal (2) disappears rapidly with increasing atom number ( $\propto 1/N$ ).

Fluorescence of the atoms trapped in the MOT was observed with avalanche photodiodes (APDs) in a single-photon counting mode with a measured photon detection efficiency of 50%. About 4% of the total fluorescent light is collected by a lens placed inside the vacuum chamber. After passing through a beam splitter and the imaging optics, the light is focused on the apertures of two cooled APDs with dark count rates below 15/s. Typical photon count rates  $R=3-20$  kHz per atom are detected, depending on the detuning  $\delta$  of the trapping laser from the atomic resonance ( $\delta/\Gamma = -8, \dots, -1$ , in terms of the natural linewidth  $\Gamma = 2\pi \times 5.2$  MHz) and on the laser intensity (typically  $15I_0$  per beam in terms of the saturation intensity  $I_0 = 1.1$  mW/cm<sup>2</sup>). At a magnetic-field gradient of 375 G/cm and background pressure of  $8 \times 10^{-11}$  Torr it is possible to observe a single trapped atom for as long as ten minutes. Well-separated discrete steps in the fluorescence signal allow us to monitor the current number of trapped atoms.

We use two techniques to record two-photon correlations. At short time scales below 20  $\mu$ s the pulses from both photodiodes are directed separately to the start and stop inputs of a time-to-amplitude converter and a multichannel analyzer. This single-stop technique has a high time resolution of better than 1 ns and provides the waiting time distribution that is proportional to the intensity correlation function if the coincidence probability within the relevant time span is much

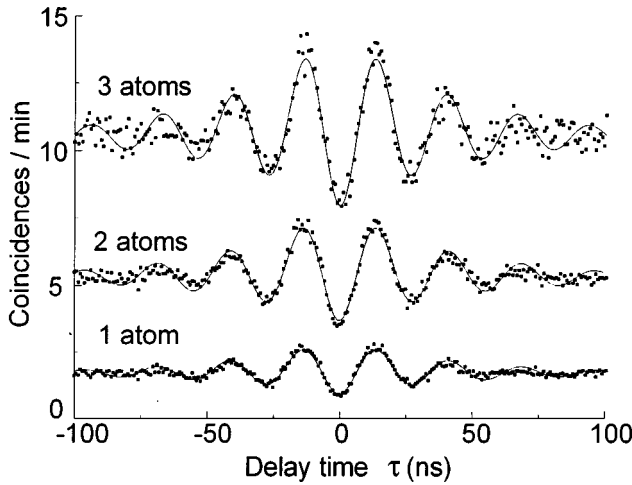


FIG. 1. Two-photon correlation in the resonance fluorescence from  $N$  atoms trapped in the MOT at the laser detuning  $\delta/2\pi = -20$  MHz. The solid line is a fit with only one fit parameter  $\Omega$  (all count rates were measured independently). The measured dependence of the Rabi frequency  $\Omega$  on the laser detuning  $\delta$  follows  $\Omega^2 = \Omega_R^2 + \delta^2 - (\Gamma/4)^2$ ,  $\Omega_R$  being the Rabi frequency at resonance. Its absolute value  $\Omega_R/2\pi = 31.1 \pm 0.2$  MHz agrees within 6% with the one determined from the measured power-broadened width of the fluorescence as a function of the trapping laser detuning.

smaller than 1. At higher count rates (or for larger time scales) a systematic error is introduced [10], since only the first detected stop photon is used for timing purposes and any subsequent stop photons are lost. This problem is eliminated by recording arrival times of all photons at time scales  $>100$  ns, which are then correlated by a computer program. Such a multiple-stop technique does not need any corrections at longer times, agrees perfectly with the single-stop results at shorter times, and allows quantitative analysis of the correlation signal amplitude.

The two-photon correlations in the fluorescence of trapped neutral atoms measured separately for different atom numbers are shown without any corrections in Fig. 1. They exhibit photon antibunching and distinctive Rabi oscillations. In the experiment the Rabi oscillations are averaged over atomic trajectories in the MOT, where the three-dimensional light interference pattern has different polarizations at different places. Despite this complex situation and the complicated multilevel structure of the cesium atom the Fourier transform of  $g^{(2)}(\tau)$  shows only one significant component. The observation suggests that due to optical pumping a trapped atom spends most of its time in the state that interacts most strongly with the local field and is forced to behave, to a good approximation, like a two-level system. The importance of local optical pumping in the MOT light field has been discussed previously in [11]. Therefore, we have analyzed the data with a simple model: a two-level atom driven by near-resonant laser radiation, whose correlation function for resonance fluorescence is given in [12]. This simple model reproduces the observed oscillations surprisingly well (Fig. 1).

Moving through the trap the atom visits various spots of the light interference pattern with different intensity and polarization [13]. The polarization of resonance fluorescence is determined by the magnetic orientation of the atom, which in

turn depends on the local light field [14] and changes on the time scale of atomic transport over an optical wavelength  $\lambda$ . Thus, in addition to correlations of the total intensity (1), one expects polarization effects [1], that is, correlation  $g_{\alpha\beta}^{(2)}$  measured between any polarization components  $\alpha$  and  $\beta$  that should strongly depend on the atomic motion and on the light-field topography. If we describe the position-dependent fluorescence intensity of the polarization component  $\alpha$  by  $I_\alpha(z)$  and the probability for the atom to be at time  $t$  at  $z$  for the initial atom position  $z(0) = z_0$  by  $f(z, z_0, t)$ , then the corresponding autocorrelation function is proportional to  $\int_{-\infty}^{\infty} dz dz_0 I_\alpha(z_0) I_\alpha(z) f(z_0, z_0, \infty) f(z, z_0, \tau)$ .

In order to gain physical insight let us start with a one-dimensional case. A pair of two circularly polarized laser beams with the same handedness (so-called  $\sigma^+\sigma^-$  case) counterpropagating along  $z$  produces a local polarization that is linear everywhere with a direction of polarization that rotates a full turn every wavelength. If we model an atom by a classical emitter with an induced dipole moment proportional to the local light field, then the intensity  $I_x$  radiated in the  $z$  direction and measured after passing through a polarizing filter oriented along  $x$  depends on the atom position  $z$  in a simple way  $I_x \propto \sin^2(kz)$ , where  $k$  is the wave number. Assuming, for example, that the atom undergoes diffusive motion with the probability distribution function of the form  $f(z, z_0, t) = \exp[-(z - z_0)^2/\xi^2(t)]/[\xi(t)\sqrt{\pi}]$ , one obtains

$$g_{xx}^{(2)}(\tau) = 1 + \frac{1}{2} e^{-k^2 \xi^2(\tau)}. \quad (3)$$

Note that the same result (3) is also valid for the autocorrelation  $g_{++}^{(2)}(\tau)$  (i.e.,  $\sigma^+$ -component correlation) measured in a standing wave produced by two counterpropagating laser beams with mutually orthogonal linear polarization ( $\text{lin} \perp \text{lin}$ ). The total intensity is constant in both configurations (there are no intensity gradients) and thus  $g^{(2)}(\tau) = 1$  (Rabi oscillations are neglected).

We have observed auto and cross correlations with surprisingly large amplitude for circular components, but no correlations for linear polarizations; see Fig. 2. Qualitative agreement of the model and the experimental data is found for the order of magnitude of the time constant. For a Cs atom at the Doppler-limit temperature (125  $\mu\text{K}$ ) it takes a time  $\lambda/v \approx 2\pi 30/\Gamma$  to pass a distance  $\lambda$ . It gives for the decay time in Eq. (3) a value of  $(kv)^{-1} \approx 1 \mu\text{s}$ . Preliminary results indicate that the decay time increases with decreasing laser intensity as one would expect.

Replacing the classical emitter by a real cesium atom can shed light on the vanishing contrast for the case of linear polarizations. A steady-state atom with transition  $F=4 \rightarrow F'=5$  driven by linear polarization ( $\sigma^+\sigma^-$  case) emits spontaneously  $\pi$ ,  $\sigma^+$ , and  $\sigma^-$  photons (quantization axes parallel to the light polarization) in a proportion 9:4:4. The linear polarization intensity in this case  $I_x \propto 4 + 9 \sin^2(kz)$  reduces the contrast in Eq. (3) by a factor of 3.6. Conversely, the  $\sigma^+$  intensity (quantization axes parallel to  $z$ ) in a one-dimensional (1D)  $\text{lin} \perp \text{lin}$  field as a function of the atom position remains fully modulated, because the atom subjected to  $\sigma^+(\sigma^-)$  light can emit only the corresponding circular polarization due to optical pumping. In

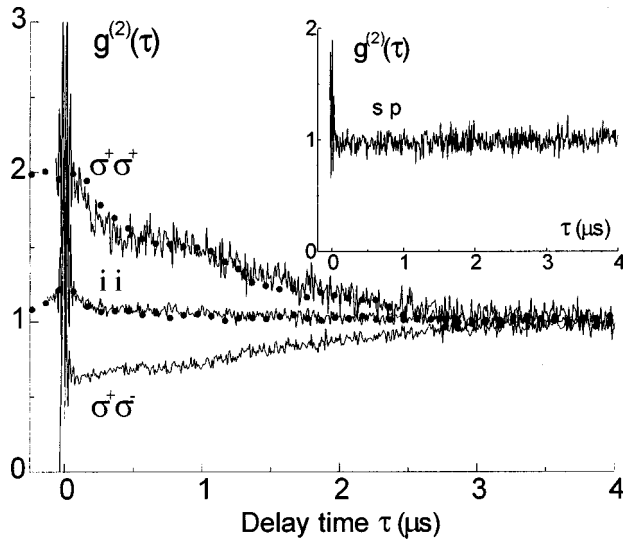


FIG. 2. Polarization correlations of a single-atom fluorescence at  $\delta/2\pi = -20$  MHz. Solid lines, single-stop measurements corrected for exponential decay; dots, multiple-stop measurements with a time resolution of 100 ns. At very short time scales a strong reflection of the Rabi oscillations described above is again visible [15]. Linear polarization  $s$  is defined as being parallel to the trap symmetry axis  $z$ ;  $p$  is orthogonal to  $s$ . The formal relation  $2g^{(2)}(\tau) = g_{++}^{(2)}(\tau) + g_{+-}^{(2)}(\tau)$  has been tested independently by directly measuring  $g^{(2)}(\tau)$  for the total intensity (ii), yielding good agreement.

the  $\text{lin} \perp \text{lin}$  case optical pumping also induces changings in the total intensity: a Cs atom driven by a linear polarized field scatters to the detector about two times less photons than in the case of circular polarization. As a result the total scattered intensity is doubly modulated in comparison with circular components explaining the different decay times (approximately a factor of 4) for intensity and polarization correlations; see Fig. 2.

The model can be extended into three dimensions, making any known field configuration analytically accessible. But intuitively it is clear that a 3D interference light pattern will show less pronounced polarization gradients [16] decreasing the contrast [17]. Note, however, that the correlations for circular polarization are much stronger,  $g_{++}^{(2)}(0) \approx 2$ , than predicted by Eq. (3), even for a fully modulated fluorescence signal. The reason for this deviation can be found in the effect of optical lattices on atomic transport in the trap. The correlation function amplitude for a  $\sigma^+$ -polarization component is given by  $g_{++}^{(2)}(0) \propto \int dz I_+^2(z) f(z, z, \infty)$ , where  $f(z, z, \infty)$  describes the probability for an atom to be at  $z$ . If the atom stays longer at places with a certain polarization of the laser field, say  $\sigma^+$  and  $\sigma^-$ , it will cause stronger fluctuations of the detected  $I_+(t)$  signal, increasing the value of  $g_{++}^{(2)}(0)$  and simultaneously decreasing the contrast of the correlations between the linear components. Thus we believe that  $g_{\alpha\beta}^{(2)}(0)$  can be used as a direct measure of the atomic localization in optical potentials, although this interpretation is still under investigation. For a quantitative analysis of the polarization correlations in the case of a standard 3D MOT it is desirable not only to have a more sophisticated theoretical model but also to experimentally control the phase relations between the six trapping laser beams. The light field topography strongly depends on these time phases [16], which are

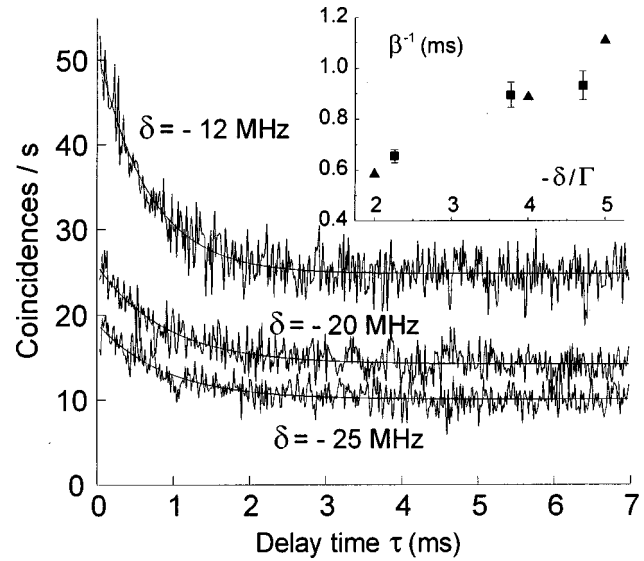


FIG. 3. Intensity autocorrelations recorded from the half image of the trap at different laser detunings  $\delta$ . The integration time was about 4 min for all measurements. Solid lines are fits according to Eq. (4). Inset: Position damping times  $\beta^{-1} = \alpha/\kappa$  as a function of laser detuning  $\delta$ .  $\square$ , our data;  $\Delta$ , from Fig. 17 in Ref. [20] multiplied by 5.2/375, the ratio of the magnetic field gradients used in two experiments.

not controlled in usual MOT experiments. Expected changes of the temperature and the damping time constant [18] as a function of the relative phases can be explored by applying our method to light configurations with well-defined and stable light field topography [19].

Note that from Eq. (3) all correlations disappear after the atom has passed a length  $\xi(t) > \lambda$  due to the stochastic nature of the atomic motion on large scales. However, information on atomic motion at extended scales can be obtained directly by spatially resolved fluorescence detection, beginning at the diffraction limit. We have generated a slowly fluctuating fluorescence signal depending on atomic position in the trap by introducing a knife edge into an intermediate trap image. Since the uncertainty in the atom position due to diffraction in the imaging system is an order of magnitude smaller than the trap size ( $1/e$  diameter of  $40 \mu\text{m}$ ), we assume that registration of a photon locates the atom in the unobstructed part of the trap volume. In this case the intensity correlation is given by  $g^{(2)}(\tau) = P(\tau)/P(\infty)$ , where  $P(\tau)$  describes the conditional probability of seeing the atom at time  $t = \tau$  after it has been seen at  $t = 0$ .

The long-range trapping force in the MOT arising from unbalanced radiation pressure due to the Zeeman detuning in the magnetic quadrupole field can be expressed as a damped harmonic force [6] with spring constant  $\kappa$  and friction parameter  $\alpha$ . Random fluctuations of the friction force may be characterized by a diffusion constant, leading to a Fokker-Planck equation for atomic motion in the trap. Introducing for convenience  $y = z\sqrt{\kappa/2k_B T}$ ,  $a^2(t) = 1 - \exp(-2\beta t)$ , and  $\beta = \kappa/\alpha$ , we have for the probability distribution  $f(y, y_0, t) = [a(t)\sqrt{\pi}]^{-1} \exp[-(y - y_0 e^{-\beta t})^2/a^2(t)]$ . The temperature  $T$  has the meaning of an average kinetic energy of the trapped atom. For the symmetrical case of a half obstructed trap the correlation function can be given analytically,

$$g^{(2)}(\tau) = 1 + \frac{2}{\pi} \frac{\arccos \sqrt{[1 + \exp(-\beta\tau)]/2}}{(1 + \langle S \rangle / \langle I \rangle)^2}, \quad (4)$$

where we included the reduction of contrast by the average stray-light intensity  $\langle S \rangle$ . We have also checked that spherical aberrations that are present in our imaging system and further reduce the contrast do not change the form of the correlation function.

The positional correlations measured at different laser detunings are shown in Fig. 3. From a fit according to Eq. (4), position damping times  $\beta^{-1}$  are found in good agreement with the data of Ref. [20] (see inset in Fig. 3). In that experiment  $\beta^{-1}$  was measured by monitoring the motion of the trap center after having introduced a small displacement using an additional magnetic field. In contrast to our noninvasive method, restrictions on experimental parameters were necessary to ensure that the situation did not deviate significantly from the steady-state dynamics.

The problem of spatial diffusion of atoms in optical lattices remains one of the difficult points in an understanding of laser cooling [21]. Correlation techniques provide in principal complete information on the atomic motion encoded in the photon statistics, and spatially resolved photon detection allows us to combine high temporal and spatial resolution. The advantage of single-atom observation has been recently demonstrated also in [22], where indications for Lévy walks were found by tracing the position of a single ion in a one-dimensional optical lattice. We have shown here that single neutral atoms can be probed as sensitively as trapped single ions.

This work was funded by the Deutsche Forschungsgemeinschaft. H. Schadwinkel, H. Leinen, K. Dästner, A. Rauschenbeutel, and K. D. Krause have contributed in the early stages of the experiment, and we have profited from discussions with G. Nienhuis on theoretical aspects.

- 
- [1] C. Jurczak *et al.*, Phys. Rev. Lett. **77**, 1727 (1996).
  - [2] S. Bali *et al.*, Phys. Rev. A **53**, 3469 (1996).
  - [3] H. J. Kimble, M. Dagenais, and L. Mandel, Phys. Rev. Lett. **39**, 691 (1977); F. Diedrich and H. Walther, *ibid.* **58**, 203 (1987).
  - [4] W. Neuhauser *et al.*, Phys. Rev. A **22**, 1137 (1980).
  - [5] Z. Hu and H. J. Kimble, Opt. Lett. **19**, 1888 (1994); F. Ruschewitz *et al.*, Europhys. Lett. **34**, 651 (1996); D. Haubrich *et al.*, *ibid.* **34**, 663 (1996).
  - [6] E. L. Raab *et al.*, Phys. Rev. Lett. **59**, 2631 (1987); for a recent review see C. G. Townsend *et al.*, Phys. Rev. A **52**, 1423 (1995).
  - [7] The dynamics of the trapped atom number (time scale of second/minute) will be discussed elsewhere.
  - [8] Roy J. Glauber, Phys. Rev. **130**, 2529 (1963); **131**, 2766 (1963).
  - [9] R. Loudon, *The Quantum Theory of Light*, 2nd ed. (Oxford University Press, New York, 1983), p. 308.
  - [10] P. B. Coates, J. Sci. Instrum., Ser. 2 **1**, 878 (1968).
  - [11] J. Javanainen, J. Opt. Soc. Am. B **10**, 572 (1993).
  - [12] H. J. Kimble and L. Mandel, Phys. Rev. A **13**, 2123 (1976).
  - [13] The measured time phase fluctuations are slower than 10 kHz; therefore at time scales of  $\mu$ s an atom “sees” a well-defined optical lattice.
  - [14] Partial depolarization due to the Hanle effect in the magnetic field is significant only for displacements from the trap center larger than 1 mm and can be neglected here.
  - [15] Polarization effects at short time scales were discussed for a simple transition in C. Cohen-Tannoudji and S. Reynaud, Philos. Trans. R. Soc. London, Ser. A **293**, 223 (1979).
  - [16] S. Hopkins and A. Durrant, Phys. Rev. A **56**, 4012 (1997).
  - [17] In the real experiment there are even more reasons to expect much less contrast, e.g., saturation effects or projection onto the observation direction.
  - [18] K. Mölmer, Phys. Rev. A **44**, 5820 (1991); A. M. Steane, M. Chowdhury, and C. J. Foot, J. Opt. Soc. Am. B **9**, 2142 (1992).
  - [19] A. Rauschenbeutel *et al.*, Opt. Commun. **148**, 45 (1998).
  - [20] M. Drewsen *et al.*, Appl. Phys. B: Lasers Opt. **59**, 283 (1994).
  - [21] T. W. Hodapp *et al.*, Appl. Phys. B: Lasers Opt. **60**, 135 (1995).
  - [22] H. Katori, S. Schlopf, and H. Walther, Phys. Rev. Lett. **79**, 2221 (1997).